APPLIED AND ENVIRONMENTAL MICROBIOLOGY, Mar. 2004, p. 1777–1786 Vol. 70, No. 3
0099-2240/04/$08.00+0 DOI: 10.1128/AEM.70.3.1777–1786.2004
Copyright © 2004, American Society for Microbiology. All Rights Reserved.

Bacterial Succession in a Petroleum Land Treatment Unit

Christopher W. Kaplan and Christopher L. Kitts*

Environmental Biotechnology Institute, California Polytechnic State University, San Luis Obispo, California 93407

Received 14 July 2003/Accepted 10 December 2003

Bacterial community dynamics were investigated in a land treatment unit (LTU) established at a site contaminated with highly weathered petroleum hydrocarbons in the C_{10} to C_{32} range. The treatment plot, 3,000 cubic yards of soil, was supplemented with nutrients and monitored weekly for total petroleum hydrocarbons (TPH), soil water content, nutrient levels, and aerobic heterotrophic bacterial counts. Weekly soil samples were analyzed with 16S rRNA gene terminal restriction fragment (TRF) analysis to monitor bacterial community structure and dynamics during bioremediation. TPH degradation was rapid during the first 3 weeks and slowed for the remainder of the 24-week project. A sharp increase in plate counts was reported during the first 3 weeks, indicating an increase in biomass associated with petroleum degradation. Principal components analysis of TRF patterns revealed a series of sample clusters describing bacterial succession during the study. The largest shifts in bacterial community structure began as the TPH degradation rate slowed and the bacterial cell counts decreased. For the purpose of analyzing bacterial dynamics, phylotypes were generated by associating TRFs from three enzyme digests with 16S rRNA gene clones. Two phylotypes associated with *Flavobacterium* and *Pseudomonas* were dominant in TRF patterns from samples during rapid TPH degradation. After the TPH degradation rate slowed, four other phylotypes gained dominance in the community while *Flavobacterium* and *Pseudomonas* phylotypes decreased in abundance. These data suggest that specific phylotypes of bacteria were associated with the different phases of petroleum degradation in the LTU.

A bioremediation project was undertaken at the Guadalupe oil field, which occupies nearly 2,700 acres of the larger Guadalupe-Nipomo Dune Complex and is located on the central California coast in San Luis Obispo and Santa Barbara Counties. Due to the viscous nature of the oil at the site a light petroleum distillate, referred to as diluent, was pumped into the wells to thin the oil for more efficient removal. This diluent was inadvertently released into the environment as pipes and storage tanks began to degrade. During site remediation, contaminated soil was stockpiled for eventual cleanup. Prior to treatment, the stockpiled soil contained an average total petroleum hydrocarbon (TPH) concentration of 2,440 mg per kg. A 3,000-cubic yard land treatment unit (LTU) was set up to investigate the feasibility of bioremediation at the site. Soil at the site is coastal dune sand and contained negligible carbon, nitrogen, and phosphorous. Therefore, basic nutrients consisting of phosphate and ammonia were added to obtain a C/N/P ratio of 100:6:1, and soil was periodically watered and tilled to a depth of 18 in. to aerate and mix nutrients. Details of LTU construction and maintenance were listed by Kaplan et al. (19).

Land treatment, an alluring method of remediation due to its effectiveness, low cost, and minimal environment impact, is a form of bioremediation whereby autochthonous soil bacteria degrade undesirable environmental waste. Three types of bioremediation are predominant in the industry today: natural attenuation, biostimulation, and bioaugmentation. The simplest method of bioremediation to implement is natural attenuation, where contaminated sites are only monitored for contaminant concentration to assure regulators that natural processes of contaminant degradation are active. Biostimulation is the process of providing bacterial communities with a favorable environment in which they can effectively degrade contaminants. When nutrients are low and the speed of contaminant degradation is an issue, the addition of nitrogen and phosphorous as well as aeration of soil will speed up the bioremediation process (17, 32, 34). In cases where natural communities of degrading bacteria are at low levels or not present, the addition of contaminant-degrading organisms, known as bioaugmentation, can speed up the process (3). Although significant research is being performed in this area, bioaugmentation is generally not practiced, since introduced bacteria usually can't compete with well-adapted autochthonous bacterial communities (24).

Many studies have looked at the chemical degradation process associated with land treatment (2, 4, 29). A common phenomenon in land treatment is a two-phase pattern of degradation characterized by an initial fast degradation phase followed by a slow degradation phase. To explain the change in degradation rates, it has been suggested that the initial fast degradation phase is mediated by bacterial utilization of bioavailable compounds and is governed by enzyme kinetics. In contrast, the slow phase may be governed by the rate of petroleum dissolution from soil particles (2, 4).

Although significant work has been published discussing the bacterial community structure and degradation kinetics associated with bioremediation of environmental contaminants, few have focused on a detailed description of bacterial community dynamics during this process. A recent report described the structure and dynamics of bacterial communities involved in bioremediation of crude oil (24). In this study, a few groups of bacteria were observed to increase in abundance in response

* Corresponding author. Mailing address: Environmental Biotechnology Institute, California Polytechnic State University, San Luis Obispo, CA 93407. Phone: (805) 756-2949. Fax: (805) 756-1419. E-mail: ckitts@calpoly.edu.

Downloaded from http://aem.asm.org/ on May 9, 2021 by guest

to oil contamination, but the paucity of samples analyzed left gaps during the first 3 weeks, when key events in bioremediation are known to occur (2, 4).

Because the fast degradation phase is where most petroleum is degraded, determining the key bacteria in this phase compared to the later, slower phase of degradation is important to a complete understanding of the degradation process. In this study, we present the characterization of an autochthonous bacterial community capable of degrading petroleum hydrocarbons after biostimulation by aeration and the addition of nitrogen and phosphorous nutrients. The sampling frequency was increased compared to other studies to better understand how the bacterial community changed during land treatment. A combination of 16S rRNA gene terminal restriction fragment (TRF; also known as TRF length polymorphism [T-RFLP]) analysis of bacterial communities using multiple enzymes and a clone library constructed from study samples allowed monitoring of relative bacterial abundance and the identification of bacterial phylotypes associated with the phases of TPH degradation.

MATERIALS AND METHODS

Sample storage, bacterial counts, and DNA extraction. One soil sample was taken from the large stockpile of soil used to fill the LTU. Five soil samples were taken from the LTU on a weekly basis after initiation of treatment until the 15th week, after which samples were taken at the 18th and 24th week. A subset of four soil samples were refrigerated on site until transported to the lab for bacterial plate counts on R2A agar (Difco, Detroit, Mich.). Soil samples for DNA extraction were collected and stored on site in a freezer until transferred to the laboratory, where they were stored at −80°C. The five soil samples from each weekly sampling were combined and mixed thoroughly, because the cost of analysis for all replicate samples was prohibitive. A set of replicates was analyzed, and heterogeneity of the resulting TRF patterns was considered minimal (data not shown). Five replicate soil extractions were performed on the combined soil to recover sufficient DNA for analysis. In a sterile weigh boat, 1 g of soil was weighed out and transferred into MoBio bead lysis tubes (Solano Beach, Calif.). The protocol given in the MoBio kit was followed for the extraction process with the following exception: cells were lysed in the Bio 101 FP-120 FastPrep machine (Carlsbad, Calif.) running at 5.0 m/s for 45 s. The isolated DNA was visualized by agarose gel electrophoresis, and quintuplet extractions were combined from each soil sample before PCR. The combined DNA was quantified by UV spectrophotometry.

PCR. Amplification of the template DNA was performed by using the 16S rRNA gene labeled primers 46f (5′-GCYTAACACATGCAAGTCGA) and 536r (5′-GTATTACCGCGGCTGCTGG), resulting in fragments of approximately 490 bp. For TRF analysis, the forward primer (46f) was labeled with the 6-carboxyfluorescein dye (Applied Biosystems, Fremont, Calif.). Reactions were carried out in triplicate with the following reagents in 50-μl reaction volumes: template DNA, 10 ng; 1× Ampli*Taq* Gold buffer (Applied Biosystems); deoxynucleoside triphosphates, 3×10^{-5} mmol; bovine serum albumin, 4×10^{-2} μg; $MgCl_2$, 1.75×10^{-4} mmol; primers 46f and 536r, 10^{-5} mmol each; Ampli*Taq* Gold DNA polymerase (Applied Biosystems), 1.5 U. Reaction temperatures and cycling for samples were as follows: 95°C for 2 min; 35 cycles of 94°C for 1 min, 46.5°C for 1 min, and 72°C for 2 min; followed by 72°C for 10 min. Products were visualized by agarose gel electrophoresis, and any inconsistent or unsuccessful reactions were discarded. Primers were removed, and amplicons were concentrated with the MoBio PCR Clean-Up kit according to the normal protocol. The triplicate reaction mixtures were combined and then quantified by UV spectrophotometry.

Amplicon digestion. Restriction enzyme reaction mixtures contained 75 ng of labeled DNA and 1.5 U of restriction endonuclease *Dpn*II, *Hae*III, or *Hha*I (New England Biolabs, Beverly, Mass.) in the manufacturer's recommended reaction buffers. Reactions were incubated for 2 h at 37°C followed by a 20-min 65°C denaturing step. Digested DNA was purified by ethanol precipitation.

TRF size determination. Precipitated DNA was dissolved in 9 μl of Hi-DI formamide (Applied Biosystems) with 0.5 μl of Genescan Rox 500 (Applied Biosystems) and Rox 550-700 (BioVentures, Murfreesboro, Tenn.) size standards. The DNA was denatured at 95°C for 4 min and rapidly cooled for 10 min in an ice slurry. Samples were run on an ABI Prism 310 genetic analyzer at 15 kV and 60°C. TRF sizing was performed using Genescan 3.1.2 software with the local Southern method and heavy smoothing (Applied Biosystems).

TRF data analysis. Sample data consisted of the peak area for each TRF peak in a TRF pattern. TRF data were normalized before analysis as discussed by Kaplan et al. (18). TRF patterns from all samples were analyzed using principal components analysis (PCA) and agglomerative hierarchical cluster analysis (AHCA). All analyses were performed on normalized data sets consisting of sample name, TRF length, and TRF peak area using S-Plus 6 (Insightful, Seattle, Wash.). TRF data from *Dpn*II-, *Hae*III-, and *Hha*I-digested samples were combined into a composite data set for analysis with PCA and AHCA. Covariance and correlation PCA were used in this analysis, but only covariance data are presented, since both methods produced similar results. Clusters described in this analysis were determined using AHCA with complete linkage. A Loess (nonparametric local regression) line was generated using Minitab 13 (Minitab, Inc., State College, Pa.) to approximate the trends present in diversity indices.

Cloning and phylogenetics. Two soil samples (days 14 and 56) were used for constructing a bacterial 16S rRNA gene clone library. Bacterial communities were amplified as stated above, except an unlabeled forward primer was used. PCR products from these samples were purified using the MoBio PCR Clean-Up kit. Cleaned PCR product was then ligated into the pCR 2.1 vector provided in the original TA cloning kit as directed by the manufacturer (Invitrogen, Carlsbad, Calif.). Ligated vector was then used to transform Epicurian Coli XL10-Gold ultracompetent cells (Stratagene, La Jolla, Calif.) according to the manufacturer's protocol. Cells were plated onto medium containing ampicillin–isopropyl-β-D-thiogalactopyranoside and grown overnight. White colonies were picked and grown overnight in Terrific broth (MoBio) containing ampicillin. Cells were pelleted, and plasmids were extracted using Quantum Prep HT/96 plasmid miniprep kits as directed by the manufacturer (Bio-Rad, Hercules, Calif.). Sequencing reaction mixtures (10 μl) contained the following: DNA, 4 μl; primer, 1.6×10^{-5} mmol; ABI Big Dye (Applied Biosystems), 4 μl; PCR water, 0.4 μl. Samples were run on an ABI 377 DNA sequencer, and the resulting sequences were analyzed using SeqManII (DNAStar, Madison, Wis.). Clone sequences were also analyzed with Chimera Check on the Ribosomal Database Project website (25). Nonchimeric sequences were tentatively identified using a BLAST search on the National Center for Biotechnology Information web page. The BLAST search matches with the highest BLAST scores were used in creating phylogenetic trees. Reference organisms and clones were aligned using ClustalX (33), and phylogenetic trees were constructed from the aligned sequences using Seqboot, DNADIST, DNAPARS, DNAML, and Consense in the Phylip version 3.6a2.1 package (13). Agreement between trees created with different methods served as a basis for evaluating accurate recreation of phylogenetic structure. Phylogenetic trees used in this paper were the result of resampling 100 jackknifed data sets with the DNAML maximum likelihood algorithm. Trees were visualized using Treeview version 1.6.5.

Database matching of TRF peaks. A database was created containing predicted TRFs for clones in this study and ~30,000 16S rRNA gene sequences from the Ribosomal Database Project (25) and GenBank; all sequences were trimmed to the correct size using in silico PCR with primers 46f and 536r and digested in silico with every commercially available restriction enzyme. Observed TRF peaks were compared to predicted TRF peaks of clones and public database sequences. Differences are commonly reported between observed TRF lengths and those predicted from sequence analysis (11, 18, 20, 22). This was compensated for by correcting for dye-based differences in the migration of ROX-labeled standard peaks and 6-carboxyfluorescein-labeled sample peaks (20). In addition, observed TRFs (from the sample) were allowed to be within ±2 bp (~4 standard deviations) of the predicted TRFs (from the database).

Nucleotide sequence accession numbers. The 16S rRNA clone sequences were submitted to the GenBank database and given accession numbers AY144191 through AY144298, AY149469 through AY149471, and AY154389 through AY154392.

RESULTS

TPH rate determination. The petroleum contaminant in this study was in the C_{10} to C_{32} range and was well weathered after up to 30 years in the soil. No benzene, toluene, ethylbenzene, xylene, or polycyclic aromatic hydrocarbon compounds were detected at any time during the study, and no volatile organic compounds were detected during air monitoring, so it is suspected that a limited amount of TPH was lost to evaporation

Downloaded from http://aem.asm.org/ on May 9, 2021 by guest

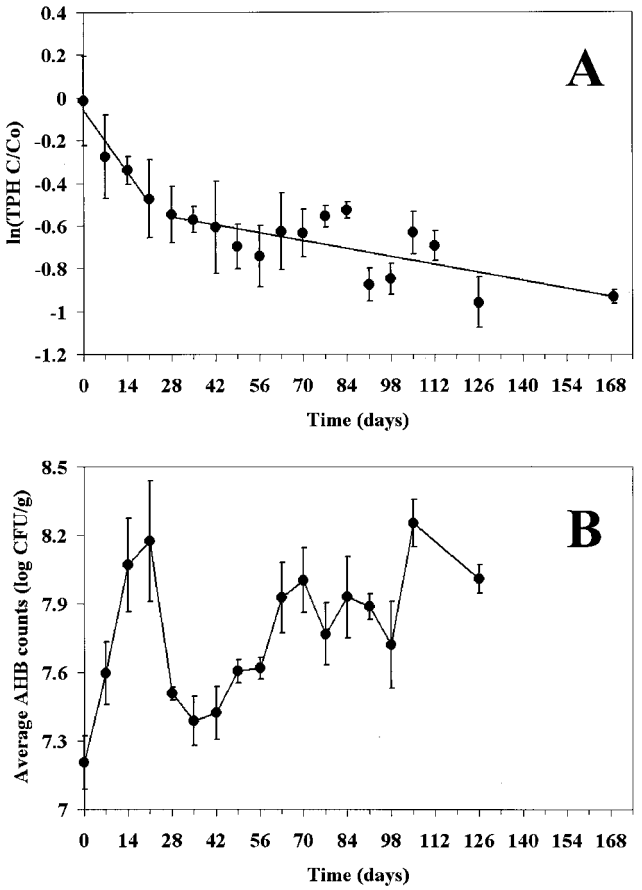

FIG. 1. Average relative TPH concentration (A) and average AHB counts (B) in the LTU.

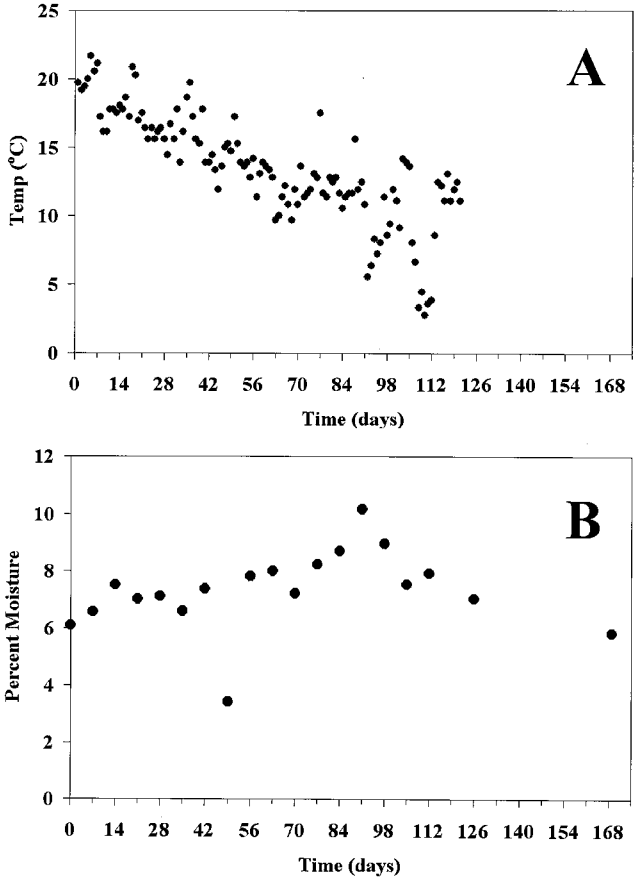

FIG. 2. Average ambient temperature (A) and soil moisture content (B) at LTU site.

(unpublished data). Attempts to fit a single first-order decay curve to the entire data set did not adequately explain (r^2 = 0.5) the changes in TPH concentration observed during the study. Consequently, a two-phase TPH degradation scheme was investigated. To determine the breakpoint in the degradation rates, regression analysis was performed on a data set broken into two groups (early and late). Sample membership within the early and late groups was varied so that all possible breakpoints were considered. The breakpoint that best fit the data in both cells put days 0 to 21 in the early group (r^2 = 0.9) and days 28 to 168 in the late group (r^2 = 0.5), indicating that a change in degradation rate may have occurred between sampling days 21 and 28 (Fig. 1A). Regression analysis indicated that the change in degradation rate was not associated with changes in ambient temperature or soil moisture (Fig. 2). By the end of the 168-day LTU project, 61% of the petroleum contamination was degraded, with 37% degraded during the first 3 weeks. The first-order degradation rate constant during the first 3 weeks of the project was -0.021 day^{-1}, an order of magnitude higher than the last 21 weeks, for which the degradation rate constant was -0.0026 day^{-1}. These rate constants compared favorably with those reported for land farming of oily sludge from a petroleum refinery, although the degradation rates were slightly higher (-0.036 day^{-1}) during the early phase and decreased less dramatically (-0.013 day^{-1}) during the late phase (2).

Bacterial counts. Aerobic heterotrophic bacterial (AHB) counts were estimated by plating quadruplicate samples onto R2A medium. A large increase in bacterial biomass was observed in the first 3 weeks of the study, from an average of 1.7 $\times$ 10^7 to 1.3 $\times$ 10^8 CFU/g. After day 21, AHB counts decreased dramatically and then began to climb again, eventually reaching 1.0 $\times$ 10^8 CFU/g at the end of the study (Fig. 1B).

Bacterial diversity. 16S rRNA gene TRF patterns were created by digesting samples with one of three tetrameric restriction endonucleases, *Dpn*II, *Hae*III, or *Hha*I. TRF patterns from *Dpn*II and *Hae*III digestions had similar numbers of TRFs on average (66.1 and 64.3, respectively), while *Hha*I had fewer (51.7). The difference in peaks produced by *Dpn*II or *Hae*III and *Hha*I was expected, since in silico digestion of 16S sequences indicates that *Dpn*II produces the greatest diversity of peaks, followed by *Hae*III and then by *Hha*I. The Shannon-Weaver diversity index (H′) and Simpson dominance index (SI′) were calculated for TRF patterns generated with each restriction enzyme. The Simpson dominance index is a useful index to contrast with Shannon-Weaver in that it weights the index towards the most abundant species present. Results for *Dpn*II and *Hae*III showed similar trends in H′ and SI′, while *Hha*I results differed slightly due to the lower diversity of peaks

Downloaded from http://aem.asm.org/ on May 9, 2021 by guest

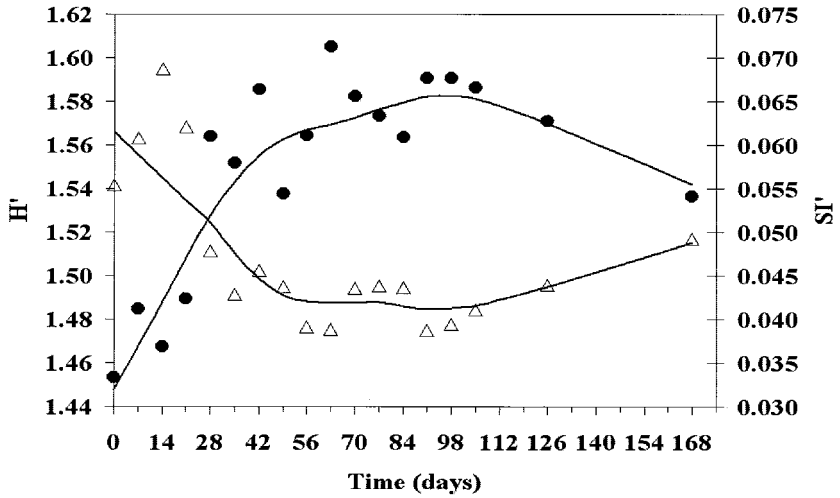

FIG. 3. Shannon-Weaver (H′) diversity index (circles) and Simpson dominance index (SI′) (triangles) based on *Dpn*II-digested samples with Loess fitted curves.

produced with this enzyme. H′ and SI′ results are shown for *Dpn*II because it produced patterns with the largest number of TRFs and produced results similar to those with *Hae*III (Fig. 3). TRF diversity (H′) increased after day 21 and remained high until the end of the study. In contrast, SI′ showed a decrease in dominance after day 21 and remained low for the remainder of the study. This suggests that during the first 3 weeks of the study a few TRFs dominated the TRF patterns and thereafter slowly decreased in abundance. Less abundant and newly detected TRFs then increased in abundance, resulting in more-evenly distributed TRF patterns with more TRFs present.

Bacterial community dynamics. Temporal changes in the bacterial community were followed using PCA and AHCA of TRF patterns. There was a clear difference in TRF patterns from samples before and after the seventh week of operations, based on a visual inspection of the raw data. PCA and AHCA showed two major groups: one group consisted of samples from early in the study (days 0 to 42), while the second group consisted of samples from later in the study (days 49 to 168). The separation between early and late clusters occurred along the first principle component (PC1), which explained 50.1% of the variation in the data (Fig. 4). Analysis of variance of the PC1 scores showed a significant difference between these two sample groups ($P < 0.05$). Coincidently, a change in soil moisture occurred around the seventh week of operation (Fig. 2).

AHCA further separated the two large groups into five smaller clusters that included three temporal shifts (Fig. 4). Cluster 1, day 0, represented a community baseline for this study due to the temporal relationship of the samples. The second cluster, days 7 to 21, represented samples taken during the fast TPH degradation phase. The first temporal shift occurred from day 0 through day 21, which coincided with fast TPH degradation and increasing bacterial counts, indicating a bloom of TPH-degrading bacteria (Fig. 1). Clusters 3 and 4 represented communities in transition after the fast degradation phase. The second temporal shift correlated with decreased bacterial counts, beginning on day 28 as TPH degradation rates changed and ending on day 49 as bacterial counts began to increase again. The third shift occurred after day 56 and continued through the final samples (days 63 to 168), which formed the fifth cluster.

Phylogenetic analysis of bacterial clones from the LTU. Days 14 and 56 were chosen to produce a clone library consisting of 115 clones later analyzed for phylogeny (Table 1). LTU clones consisted of four large groups and two smaller groups. Five groups were used to create phylogenetic trees: *Cytophaga-Flavobacterium-Bacteroides* (CFB), α-*Proteobacteria*, β-*Proteobacteria*, γ-*Proteobacteria*, and gram positives. CFB clones comprised the largest group in the study, although most came from day 14. The majority of the remaining clones were in the α-, β-, and γ-*Proteobacteria* groups. The four gram-positive clones came from day 56. No tree was made for the four ε-*Proteobacteria* clones, all from day 14, since they were not identified in TRF patterns.

No large clusters of clones were present in the α-*Proteobacteria*, indicating a broad diversity in this group. Despite this diversity, the similar number of clones from both samples indicated a constant presence and a potentially important role for this group (Table 1). The β-*Proteobacteria* clones had two major groups. Group 1 was associated with *Azoarcus*, while group 2 was associated with *Alcaligenes* and *Bordetella*.

The γ-*Proteobacteria* clones had a few significant clusters. Two clones (LTUB00356 and LTU0B1856) showed a close relationship to *Rhodanobacter lindaniclasticus*, a recently described lindane degrader (28). A large group of clones was associated with *Thermomonas heamolytica*, an organism related to *Stenotrophomonas* and *Xanthomonas* (7). The largest cluster of γ-*Proteobacteria* clones was associated with methane-oxidizing genera, *Methylococcus* and *Methylobacter* (clones LTUG017, LTUG034, LTUG036, LTUG071, and LTUG094). Clones LTUG00856 and LTUG08856 were closely associated with *Pseudomonas*, a genus known to degrade petroleum. Another cluster of clones, including LTUG005, LTUG024, LTUG01456, and LTUG07556, was loosely associated with *Nitrosococcus*, a genus known to oxidize ammonia. Due to the low bootstrap values within this section of the γ-*Proteobacteria* tree, clones associated with *Pseudomonas*, *Nitrosococcus*,

Downloaded from http://aem.asm.org/ on May 9, 2021 by guest

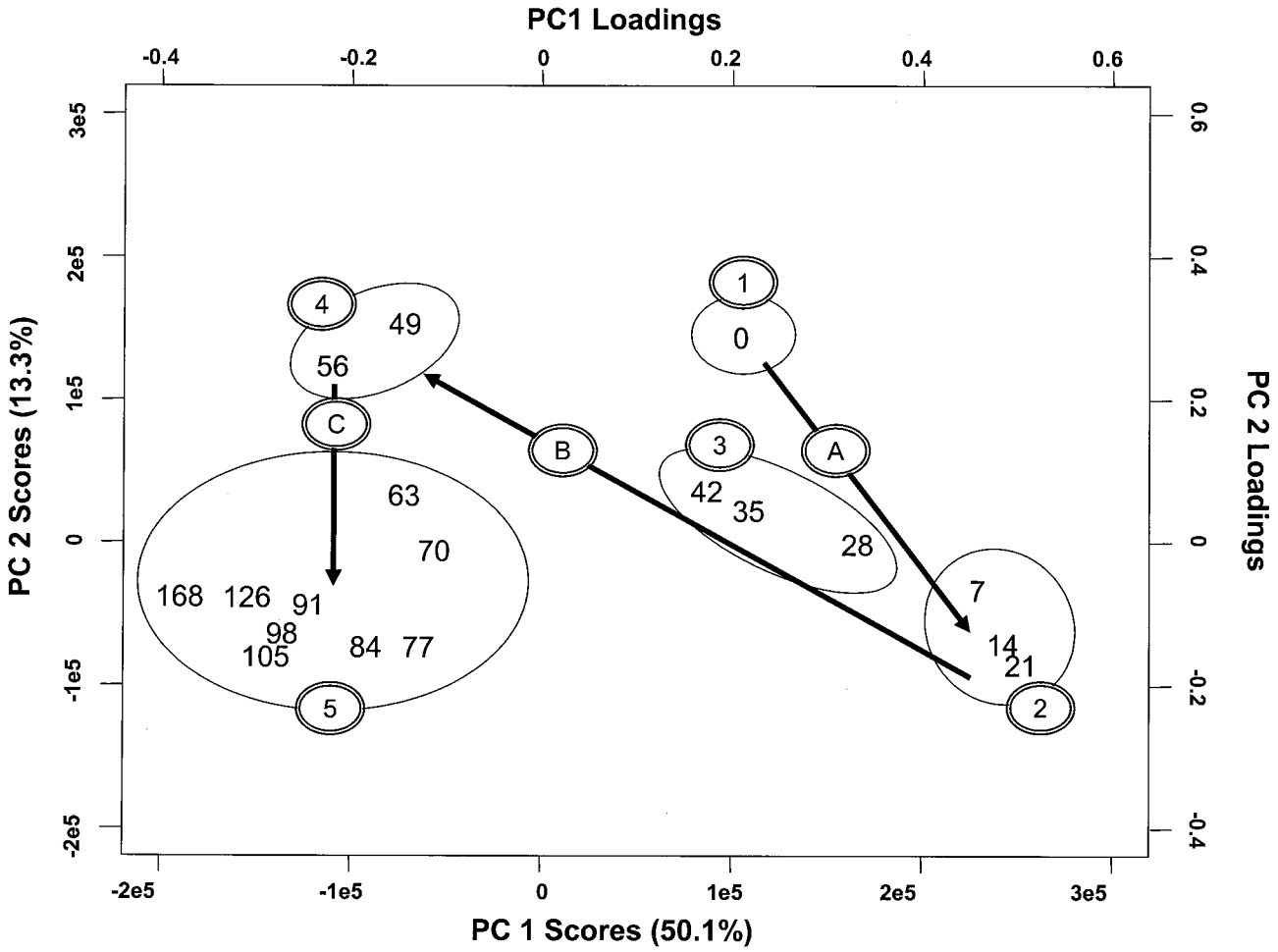

FIG. 4. PCA of combined enzyme TRF data from LTU samples. Each sample is labeled with the number of the day on which the sample was collected. Clusters determined by AHCA are labeled with numbers, and transitions between clusters are labeled with letters and arrows.

Methylobacter, and *Methylococcus*, which shared the same TRF peaks with all three enzymes, were referred to as *Pseudomonas*, the highest branch in that section of the tree.

A majority of the CFB clones were associated with *Flavobacterium* (92.3%), a genus known to degrade petroleum (5). Of these clones, 83% shared the same TRF peaks with all three enzymes. Other clones in the CFB cluster were associated with *Bacteroides* (LTUCFB047 and LTUCFB090), *Planktomyces* (LTUP05356 and LTUP07056), and *Neochlamydia* (LTUNC02956, LTUNC08556, LTUNC09456, and LTUNC09656). *Neochlamydia* organisms have been reported as endoparasites of amoebae and may indicate the presence of microeukaryotes in the LTU soil (16).

Clones within the gram-positive group were associated with *Microbacterium* (LTUGr00156 and LTUGr002356) and *Mycobacterium* (LTUGr07856).

TABLE 1. Phylogenetic group representation in two clone libraries

Phylogenetic group	No. of clones (%)	
	Day 14	Day 56
α-*Proteobacteria*	11 (17.5)	8 (15.4)
β-*Proteobacteria*	9 (14.3)	15 (28.8)
Cytophaga-Flavobacterium-Bacteroides	26 (41.3)	3 (5.8)
ε-*Proteobacteria*	4 (6.3)	0 (0)
γ-*Proteobacteria*	13 (20.6)	18 (34.6)
Gram positive	0 (0)	8 (15.4)
Total	63 (100)	52 (100)

Dynamics of dominant phylotypes during land treatment. To better understand the temporal shifts shown by PCA (Fig. 4), bacterial phylotypes were identified by associating TRFs observed in TRF patterns with predicted TRFs from the day 14 and day 56 clone libraries and public databases. TRF peaks were first grouped into TRF sets (Table 2). Each TRF set consisted of three TRF peaks, one from each enzyme digest, which had similar temporal profiles (Fig. 5) and PCA loadings (Table 2). TRF sets that did not have similar temporal profiles and PCA loadings were not carried forward. Eleven TRF sets were matched to phylotypes, and their abundance was tracked in the context of the whole community by averaging the three TRF peak areas for each TRF set. These 11 phylotypes represented the dominant features in TRF patterns, accounting for an average of 40% of the total area in TRF patterns.

Three phylotypes had a large abundance during the fast

Downloaded from http://aem.asm.org/ on May 9, 2021 by guest

TABLE 2. TRF and clone data used to identify TRF sets and assign a phylotype

TRF set	Phylotype	Enzyme	TRF (bp)		PCA loadings[e]		Matching clones
			Predicted[a]	Observed	PC1	PC2	
1	*Flavobacterium*	*Dpn*II	253	252	0.28	−0.25	LTUCFB (00314, 01914, 02514, 02914, 03914, 04314, 04614, 05714, 05914, 06314, 06914, 07414, 08014, 08314, 08614, 08814, 100144, 10148, 11314, 11414, 02256, 04256, 08156)
		*Hae*III	479	473	0.38	−0.30	
		*Hha*I	52	49	0.21	−0.19	
2	*Pseudomonas*	*Dpn*II	229	228	0.18	0.14	LTUG (00514, 01714, 02414, 03414, 03614, 07114, 09414, 00856, 01456, 07556, 08856)
		*Hae*III	162	160	0.07	0.16	
		*Hha*I	169	167	0.13	0.12	
3	*Azoarcus* 2	*Dpn*II	241	239	0.05	0.04	LTUB (01614, 03514, 09114)
		*Hae*III	174	173	0.01	0.03	
		*Hha*I	181	179	0.04	0.02	
4	*Alcaligenes*	*Dpn*II	160	159	−0.04	0.06	LTUB (00656, 03456, 03656, 04056, 04556, 05156, 05556, 06056, 07756, 08956, 09156)
		*Hae*III	113	111	−0.03	0.03	
		*Hha*I	29	ND[f]	ND	ND	
5	*Microbacterium*	*Dpn*II	76	73	−0.02	0.03	LTUGr07856
		*Hae*III	29	ND	ND	ND	LTUGr07856
		*Hha*I	331	330	−0.03	0.04	
6	*Bacteroides*	*Dpn*II	455	451	0.00	0.14	
		*Dpn*II	455	453	0.01	−0.02	LTUCFB04714, LTUCFB09014
		*Hae*III	226	225	0.01	0.11	
		*Hha*I	63	60	0.03	0.05	
7	α-*Proteobacteria*	*Dpn*II	203	201	−0.05	0.03	
		*Hae*III	155	154	−0.04	0.00	LTUA01556
		*Hha*I	434	430	−0.07	0.02	
8	*Azoarcus* 1	*Dpn*II	233	232	−0.08	0.04	
		*Hae*III	166	167[b]	−0.10	−0.04	LTUB (00214, 09814, 11114, 04856, 05656)
		*Hha*I	173	172	−0.04	0.00	
9	*Rhodanobacter*	*Dpn*II	83	80	−0.08	−0.05	
		*Hae*III	168	167[b]	−0.10	−0.04	LTUG00356, LTUG01856
		*Hha*I	175	173[c]	−0.20	−0.21	
10	Unknown	*Dpn*II	239[d]	237	−0.15	−0.22	
		*Hae*III	223[d]	224	−0.13	−0.20	No clone match
		*Hha*I	194[d]	193	−0.12	−0.18	
11	*Thermomonas*	*Dpn*II	235	233	−0.23	−0.08	
		*Hae*III	221	220	−0.17	−0.11	LTUG (00414, 02014, 07814, 09614, 04156, 07956, 08356)
		*Hha*I	175	173[c]	−0.20	−0.21	

[a] Predicted from clone sequence.
[b] *Hae*III 167 represents *Rhodanobacter* and *Azoarcus* 1.
[c] *Hha*I 173 represents *Thermomonas* and *Rhodanobacter.*
[d] Predicted from database sequences.
[e] Standard deviation = 0.04.
[f] ND, not detected (predicted TRF outside detection range of 36 to 600 bp).

degradation phase of the LTU project (Fig. 5A to C). TRF set 1, associated with *Flavobacterium* clones (Fig. 5A; Table 2), had large positive loadings along PC1, indicating these TRFs had a large influence on the separation of early and late samples. TRF set 1 also had large negative loadings along PC2, indicating the importance of these peaks in the separation of cluster 2 (days 7 to 21) from cluster 1 (day 0) and cluster 3 (days 28 to 42) in the early samples. *Flavobacterium* TRF peak area increased dramatically during the first 21 days, peaking at a high of 19.7%. *Flavobacterium* peak area slowly declined after day 14, reaching a low 3.7% on day 49 and 5.3% by the end of the study. The abundance of *Flavobacterium* in the LTU as depicted by TRF area was also reflected in the number of *Flavobacterium* clones sequenced (Table 2). Interestingly, *Flavobacterium* was detected at very low levels in a pretreatment sample (0.1%), in contrast to its large abundance throughout the rest of the project. TRF set 2, associated with *Pseudomonas* clones (Fig. 5B; Table 2), had large positive loadings along both PC1 and PC2, indicating influence on separating day 0 from days 7 to 42 in the early samples. *Pseudomonas* TRF peak area showed a rapid decrease from an average of 10.0% on day 0 to 3.9% on day 49. The decreasing trend ended after day 49, with *Pseudomonas* returning to pretreatment levels, approximately 2% of total peak area. TRF set 3, associated with *Azoarcus* 2 clones, had a similar trend, decreasing from 3.2% at day 0 to 0.7% by day 21 (Fig. 5C). Trends in TRF peak area for *Flavobacterium*, *Pseudomonas*, and *Azoarcus* 2 were similar to the trend in TPH concentration during the study. Regression analysis showed that the area of TRFs assigned to *Flavobacterium* from day 7 to day 168 had a positive correlation with relative TPH concentration ($P < 0.05$). The *Pseudomonas* and *Azoarcus* 2 TRF peak areas also had positive correlations with TPH concentration throughout the study ($P < 0.01$).

Four TRF peak sets had a large abundance during the slow degradation phase of the LTU project (Fig. 5H to K). TRF set 11 was associated with *Thermomonas* clones (Fig. 5K; Table 2) and had the largest negative loadings along PC1 and large negative loadings along PC2. TRF sets 9 and 10, associated

Downloaded from http://aem.asm.org/ on May 9, 2021 by guest

Downloaded from http://aem.asm.org/ on May 9, 2021 by guest

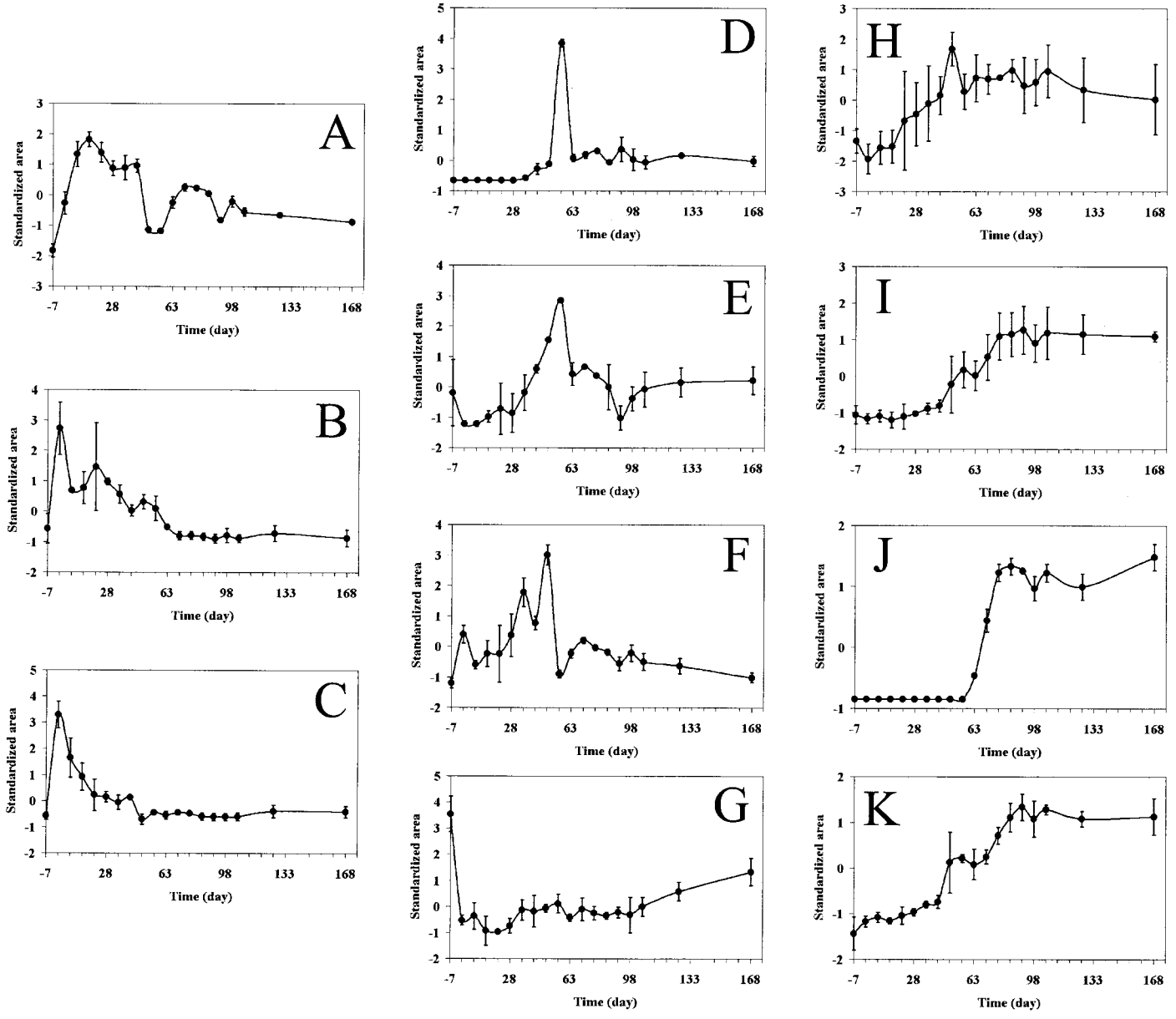

FIG. 5. Average standardized area of LTU TRF sets. Error bars indicate variation of standard error between the areas produced by enzymes *Dpn*II, *Hae*III, and *Hha*I. (A) *Flavobacterium*; (B) *Pseudomonas*; (C) *Azoarcus* 2; (D) *Alcaligenes*; (E) *Microbacterium*; (F) *Bacteroides*; (G) α-*Proteobacteria*; (H) *Azoarcus* 1; (I) *Rhodanobacter*; (J) the unknown; (K) *Thermomonas*. Average standardized area for each TRF peak was calculated by subtracting the mean TRF area from the TRF area at each time point and dividing by the standard deviation of the TRF peak area.

with *Rhodanobacter* clones and the unknown phylotype, also had large negative loadings along PC1 and PC2 (Fig. 5I and J; Table 2). The large negative loadings along both PCs indicated their importance in separating cluster 5 (days 63 to 168) from the rest of the samples. TRF set 8, associated with *Azoarcus* 1 clones, had negative loadings along PC1, indicating its importance to the separation of slow-degradation-phase samples from fast-degradation-phase samples (Fig. 5H; Table 2). *Thermomonas* and *Rhodanobacter* TRF peak area had an increasing trend, beginning with lows of 1.4 and 0.7%, respectively, on day 0, to highs of 9.6 and 5.7% on day 91. TRF set 10, labeled unknown since it lacked matching clones, remained undetected until day 63 (1.0%) and then dramatically increased to a high of 6.1% by the end of the study. Two sequences from public databases produced matching TRFs, but both were from uncultured organisms and the accompanying reports were not published. *Azoarcus* 1 TRF peak area gradually increased from a low of 1.8% at day 0 to a high of 5.7% on day 49, after which its abundance remained relatively constant. Regression analysis showed that TRF peak area associated with *Thermomonas*, the unknown, and *Rhodanobacter* had negative correlations with TPH ($P < 0.05$).

TRF sets 4 through 7 all had relatively small PCA loadings, indicating a minimal influence of these TRF sets on the creation of sample clusters (Table 2). However, abundance profiles and association with clones indicated that these TRF sets represented dominant members of the community (Fig. 5D to G; Table 2). TRF sets 4, 5, and 6, associated with *Alcaligenes*, *Microbacterium*, and *Bacteroides* clones, respectively, peaked in abundance on days 49 and 56 during the transition from fast to slow degradation phases (Fig. 5D to F). Assigning a phylotype was most difficult with TRF set 7. Four clones had TRFs in common with two of the enzymes in TRF set 7 (021, 02856, 03356, and 05256), while only one clone (01556) had all three TRFs in the set. In addition, the five clones did not cluster on the α-*Proteobacteria* phylogenetic tree. This made tracking TRF set 7 difficult, because inconsistent overlap within the phylotype disrupted the normalized abundance profiles of some enzyme digests (Fig. 5H). In spite of these difficulties, TRF set 7 served as a proxy for tracking α-*Proteobacteria* during the study. TRF set 7 was most abundant in the pretreatment sample (12%) but decreased dramatically to 3.4% on day 0. As the study progressed, there was a slow increase in α-*Proteobacteria* TRF peak area, reaching 7.4% at the end of the project. The consistent presence of these organisms in the LTU attests to their pervasive nature in the soil community.

DISCUSSION

Bacterial community dynamics in relation to petroleum concentration. The key elements in the land treatment process are the bacteria in the soil whose cellular machinery is responsible for bioconversion of contaminants. The contamination at the Guadalupe site existed undetected for an estimated 10 to 30 years, which gave ample time for bacterial communities to adapt (1, 24) and take advantage of the readily available carbon sources in petroleum. Conditions created in the LTU provided an environment conducive to the rapid degradation of available TPH. A two-phase pattern of petroleum degradation was observed during the project and was typical of that in contaminated soils undergoing land treatment (2, 4). Although the amount of TPH at this site was low when compared to other studies, Admon et al. showed that the level of contamination does not affect this two-phase pattern (2). Current data support the theory that the fast phase of petroleum degradation is limited by the microbial degradation rate of free TPH, while the slow phase is limited by the much slower desorption rate of soil-sequestered TPH.

Dominant members of the bacterial community were tracked during the project using TRF analysis and a clone library to generate 11 bacterial phylotypes (Fig. 5; Table 2). TRF patterns separated into five PCA clusters that reflected the TPH degradation phases and trends in AHB counts, SI′ and H′ (Fig. 1, 3, and 4). Clusters 1 and 2 were associated with the fast degradation phase, increasing AHB counts, and high SI′ and low H′ values during the first 21 days of the project, indicating a bloom of fast-growing petroleum degraders in the bacterial community. The *Flavobacterium*, *Pseudomonas*, and *Azoarcus* 2 phylotypes were most abundant during this fast degradation phase. Because TPH was by far the most abundant C source available in this soil, it was expected that the dominant phylotypes should have some relationship to TPH degradation. This was reflected in the positive correlation of the abundance of these phylotypes with TPH concentration as well as literature reports on the physiology of these genera (see below).

PCA clusters 3 and 4 reflected a transition out of the fast degradation phase that began with an abrupt decrease in AHB counts and SI′ and an abrupt increase in H′ and ended with a decrease in ambient temperature and transient drop in soil moisture (Fig. 1 to 3). The drop in soil moisture between days 35 and 49 was in response to a hot period of offshore winds that left a dry crust of soil on the surface. This crust was mixed into the soil by tilling before sampling. *Alcaligenes*, *Microbacterium*, and *Bacteroides* phylotypes were most abundant during this phase, although their overall abundance was low throughout the study. A large increase in abundance of these phylotypes was associated with the drop in soil moisture around day 49 (Fig. 2B and 5D to F).

Cluster 5 was associated with the stable slow degradation phase, where SI′ was low and H′ was high and AHB counts increased slowly, indicating the establishment of a stable, slowly growing community fed by the slow desorption of petroleum from the soil or other nutrients present in the soil. *Azoarcus* 1, *Thermomonas*, the unknown, and *Rhodanobacter* phylotypes were most abundant during this phase.

Significance of bacterial phylotypes in LTU. The *Flavobacterium* phylotype was of particular interest in this study, due to a high abundance during the first 3 weeks and its positive correlation with TPH levels (Fig. 1A and 5A). A rapid increase in bacterial counts was observed during the first 21 days, the same period that *Flavobacterium* increased in relative abundance, suggesting that these bacteria contributed to the increase in AHB counts during this period. The rapid increase in *Flavobacterium* was most likely due to favorable conditions established by the addition of nutrients and aeration of the LTU soil. *Flavobacterium* was less abundant in the pretreatment stockpile, where nutrients were low and oxygen was limited (data not shown). The presence of *Flavobacterium* in the community is unsurprising, since this genus has a body of work

Downloaded from http://aem.asm.org/ on May 9, 2021 by guest

supporting its importance in the bioremediation of hydrocarbon-contaminated soils. As one of the first reported bacterial isolates capable of degrading petroleum products, *Flavobacterium* is well known as a petroleum degrader. Atlas and Bartha isolated a *Flavobacterium* sp. capable of degrading 57% of a light crude oil supplement in 12 days of an aerobic microcosm experiment (5). Recent studies have found *Flavobacterium* spp. capable of degrading fluorobenzene (8), chlorinated hydrocarbons (10, 26), phenol (35), polychlorinated biphenyls (31), nylon (21), and parathion (27). MacNaughton et al. showed an increase in *Flavobacterium* abundance during an artificial oil spill, attesting to its ability to respond to hydrocarbons in the environment (24). These results suggest that the aerobic conditions provided by extensive tilling of the LTU soil contributed to the stimulation of this phylotype, thus initiating an increase in bacterial counts and a decrease in TPH levels.

The *Pseudomonas* phylotype, including the closely related genera *Pseudomonas*, *Nitrosococcus*, *Methylococcus*, and *Methylobacter*, was abundant during the fast degradation phase and correlated with TPH concentration. The breadth of genera present in this phylotype makes identification of specific bacteria difficult. Two clones associated with this TRF set matched well with the fluorescent pseudomonad cluster (Table 2). The presence of *Pseudomonas* in the LTU was unsurprising, since this genus is well described as a petroleum degrader, similar to *Flavobacterium*. Bacteria in the genera *Pseudomonas* have the ability to utilize a diverse range of substrates, including those found in petroleum (12, 15). A large amount of work has been performed on the alkane oxidation genes in *Pseudomonas*, which allow bacteria with these genes to grow on alkanes as a sole carbon source (9). The presence of *Nitrosococcus* may have been in response to ammonia addition at the beginning of the study. While it is difficult to explain the presence of *Methylococcus* and *Methylobacter*, it is possible that methane generated in the untilled lower levels of the LTU was being degraded in the aerobic upper layers by these organisms.

The *Azoarcus* 2 phylotype showed a trend similar to that of *Flavobacterium* and *Pseudomonas*. Reports show that *Azoarcus* spp. can degrade benzene, toluene, ethylbenzene, and xylene compounds (14, 30), suggesting they may play a role in TPH degradation. The role of *Azoarcus* 2 in the LTU is interesting, since this phylotype decreased in abundance while the *Azoarcus* 1 phylotype increased. It appears that these two phylotypes of *Azoarcus* had different physiological requirements.

The phylotypes associated with *Alcaligenes*, *Microbacterium*, and *Bacteroides* remained relatively low and stable throughout the bioremediation process except for a temporary increase on days 49 and 56. Species in these genera have been reported as petroleum hydrocarbon degraders (6, 15, 23, 36) and, thus, the phylotypes were candidates for a significant role in TPH degradation in the LTU; yet, the low abundance of these phylotypes may suggest a negligible role in TPH degradation. While the low relative abundance of these phylotypes may be the result of PCR bias, the important factor in distinguishing phylotypes responsible for the fast TPH degradation rate at the beginning of the study was a positive correlation with TPH concentration, as observed for the *Flavobacterium*, *Pseudomonas*, and *Azoarcus* 2 phylotypes. The stable numbers of *Alcaligenes*, *Microbacterium*, and *Bacteroides* organisms and lack of response to petroleum concentration indicate that they did not contribute significantly to the fast TPH degradation rate seen in the first 3 weeks of LTU operation but may have contributed to degradation at some level.

Three of the slow-degradation-phase phylotypes were associated with either new genera (*Rhodanobacter* and *Thermomonas*) that had little or no information about their physiology in relation to petroleum degradation or a phylotype (unknown) associated with unidentified bacterial sequences from GenBank. Both *Rhodanobacter* and *Thermomonas* live under aerobic conditions and are related to *Pseudomonas*, *Xanthomonas*, and *Stenotrophomonas*, all known hydrocarbon degraders. The unknown phylotype was interesting due to its strong association with the slow phase of TPH degradation. Further cloning from a sample where the unknown is more abundant may provide a sequence which would allow for a phylogenetic analysis of clones associated with this phylotype and a potential function for this phylotype in the LTU.

During data analysis it was observed that there was an apparently high abundance of gram-negative bacteria in this study and that this could be the result of extraction bias. However, the extraction method used in this study was also used to investigate the diversity of bacteria in rat fecal samples and revealed a bacterial community dominated by gram-positive bacteria (18), suggesting that gram-negative bacteria did in fact dominate the LTU soils.

The significance of this work is the description of the succession dynamics of dominant bacterial phylotypes correlated with the degradation of weathered petroleum hydrocarbons in the C_{10} to C_{32} range during land treatment. Based on our analysis of the bacterial community, it appears that a major portion of petroleum degradation is carried out by a few species represented by *Flavobacterium*, *Pseudomonas*, and *Azoarcus* 2 phylotypes. Once the readily available free petroleum in the soil had been depleted, these bacteria decreased in relative abundance and remained at a level where their numbers could be sustained, and petroleum continued to be degraded as it was slowly released from the soil particles. As the dominant petroleum degraders waned, other phylotypes present at lower levels, perhaps also petroleum degraders, increased in relative abundance. The trend from a lower-diversity, high-dominance community to a higher-diversity low-dominance community mirrors succession in other systems where disturbance alters the environment and the organisms adapt over time to the changed conditions. Land treatment during the study involved extensive soil tilling, drying and wetting events, and nutrient addition that likely contributed to the formation of an initial community structure dominated by fast-growing *Flavobacterium* and *Pseudomonas* phylotypes. Shannon-Weaver and Simpson dominance indices corroborated this interpretation of events, showing high dominance and low diversity during the fast degradation phase (Fig. 3). It appears *Flavobacterium* in particular was enriched by these activities, as demonstrated by its increased relative abundance during the first 3 weeks of LTU operation.

ACKNOWLEDGMENTS

This work was supported by the generous contributions of the UNOCAL Corporation, whom we thank for the opportunity to conduct research at their site and for the support of their staff in accomplishing the common goal of a cleaner environment.

Downloaded from http://aem.asm.org/ on May 9, 2021 by guest

We also thank everyone at the Environmental Biotechnology Institute, past and present, who contributed to successful completion of the LTU project.

REFERENCES

1. **Abed, R. M. M., N. M. D. Safi, J. Köster, K. de Beer, Y. El-Nahhal, J. Rullkötter, and F. Garcia-Pichel.** 2002. Microbial diversity of a heavily polluted microbial mat and its community changes following degradation of petroleum compounds. Appl. Environ. Microbiol. **68:**1674–1683.
2. **Admon, S., M. Green, and Y. Avnimelech.** 2001. Biodegradation kinetics of hydrocarbons in soil during land treatment of oily sludge. Bioremediat. J. **5:**193–209.
3. **Al-Awadhi, N., R. Al-Daher, A. ElNavavy, and M. T. Balba.** 1996. Bioremediation of oil-contaminated soil in Kuwait: landfarming to remediate oil-contaminated soil. J. Soil Contam. **5:**243–260.
4. **Alexander, M.** 2000. Aging, bioavailability, and overestimation of risk from environmental pollutants. Environ. Sci. Technol. **34:**4259–4265.
5. **Atlas, R. M., and R. Bartha.** 1972. Degradation and mineralization of petroleum by two bacteria isolated from coastal waters. Biotechnol. Bioengin. **14:**297–308.
6. **Baggi, G., and M. Zangrossi.** 1999. Degradation of chlorobenzoates in soil suspensions by indigenous populations and a specialized organism: interaction between growth and non-growth substrates. FEMS Microbiol. Ecol. **29:**311–318.
7. **Busse, H. J., P. Kampfer, E. R. Moore, J. Nuutinen, I. V. Tsitko, E. B. M. Denner, L. Vauterin, M. Valens, R. Rossello-Mora, and M. S. Salkinoja-Salonen.** 2002. *Thermomonas haemolytica* gen. nov., sp. nov., a γ-proteobacterium from kaolin slurry. Int. J. Syst. Bacteriol. **52:**473–483.
8. **Carvalho, M. F., C. C. T. Alves, M. I. M. Ferreira, P. De Marco, and P. M. L. Castro.** 2002. Isolation and initial characterization of a bacterial consortium able to mineralize fluorobenzene. Appl. Environ. Microbiol. **68:**102–105.
9. **Chakrabarty, A. M., G. Chou, and I. C. Gunsalus.** 1973. Genetic regulation of octane dissimulation plasmids in Pseudomonas. Proc. Natl. Acad. Sci. USA **70:**1137–1140.
10. **Chaudhry, G. R., and G. H. Huang.** 1998. Isolation and characterization of a new plasmid from a *Flavobacterium* sp. which carries the genes for degradation of 2,4-dichlorophenoxyacetate. J. Bacteriol. **170:**3897–3902.
11. **Clement, B. G., L. E. Kehl, K. L. DeBord, and C. L. Kitts.** 1998. Terminal restriction fragment patterns (TRFPs), a rapid, PCR-based method for the comparison of complex bacterial communities. J. Microbiol. Methods **31:** 135–142.
12. **Esteve-Nunez, A., A. Caballero, and J. L. Ramos.** 2001. Biological degradation of 2,4,6-trinitrotoluene. Microbiol. Mol. Biol. Rev. **65:**335–352.
13. **Felsenstein, J.** 1989. PHYLIP—phylogeny inference package (version 3.2). Cladistics **5:**164–166.
14. **Fries, M. R., J. Zhou, J. Chee-Sanford, and J. M. Tiedje.** 1994. Isolation, characterization, and distribution of denitrifying toluene degraders from a variety of habitats. Appl. Environ. Microbiol. **60:**2802–2810.
15. **Greene, E. A., J. G. Kay, K. Jaber, L. G. Stehmeier, and G. Voodouw.** 2000. Composition of soil microbial communities enriched on a mixture of aromatic hydrocarbons. Appl. Environ. Microbiol. **66:**5282–5289.
16. **Horn, M., M. Wagner, K.-D. Muller, E. N. Schmid, T. R. Fritsche, K.-H. Schleifer, and R. Michel.** 2000. *Neochlamydia hartmannellae* gen. nov, sp. nov. (*Parachlamydiaceae*), an endoparasite of the amoeba *Hartmannella vermiformis.* Microbiology **146:**1231–1239.
17. **Huesemann, M. H., and M. J. Truex.** 1996. The role of oxygen diffusion in passive bioremediation of petroleum contaminated soils. J. Hazard. Mater. **51:**93–113.
18. **Kaplan, C. W., J. C. Astaire, M. E. Sanders, B. S. Reddy, and C. L. Kitts.** 2001. 16S ribosomal DNA terminal restriction fragment pattern analysis of bacterial communities in feces of rats fed *Lactobacillus acidophilus* NCFM. Appl. Environ. Microbiol. **67:**1935–1939.
19. **Kaplan, C. W., B. G. Clement, A. Hamrick, R. W. Pease, C. Flint, R. J. Cano, and C. L. Kitts.** 2003. Complex co-substrate addition increases initial petroleum degradation rates during land treatment by altering bacterial community physiology. Remediation **13:**61–78.
20. **Kaplan, C. W., and C. L. Kitts.** 2003. Variation between observed and true terminal restriction fragment (TRF) length is dependent on true TRF length and purine content. J. Microbiol. Methods **54:**121–125.
21. **Kato, K., K. Ohtsuki, Y. Koda, T. Maekawa, T. Yomo, S. Negoro, and I. Urabe.** 1995. A plasmid encoding enzymes for nylon oligomer degradation: nucleotide sequence and analysis of pOAD2. Microbiology **141:**2585–2590.
22. **Kitts, C. L.** 2001. Terminal restriction fragment patterns: a tool for comparing microbial communities and assessing community dynamics. Curr. Issues Intest. Microbiol. **2:**17–25.
23. **Lai, B., and S. Khanna.** 1996. Degradation of crude oil by *Acintobacter calcoaceticus* and *Alcaligenes oderans*. J. Appl. Bacteriol. **81:**355–362.
24. **MacNaughton, S. J., J. R. Stephen, A. D. Venosa, G. A. Davis, Y. Chang, and D. C. White.** 1999. Microbial population changes during bioremediation of an experimental oil spill. Appl. Environ. Microbiol. **65:**3566–3574.
25. **Maidak, B. L., J. R. Cole, T. G. Lilburn, C. T. Parker, Jr., P. R. Saxman, R. J. Farris, G. M. Garrity, G. J. Olsen, T. M. Schmidt, and J. M. Tiedje.** 2001. The RDP-II (Ribosomal Database Project). Nucleic Acids Res. **29:**173–174.
26. **Mannisto, M. K., M. A. Tiirola, M. S. Salkinoja-Salonen, M. S. Kulomaa, and J. A. Puhakka.** 1999. Diversity of chlorophenol-degrading bacteria isolated from contaminated boreal groundwater. Arch. Microbiol. **171:**189–197.
27. **Mulbry, W. W., P. C. Kearney, J. O. Nelson, and J. S. Karns.** 1987. Physical comparisons of parathion hydrolase plasmids from *Pseudomonas diminuta* and *Flavobacterium* sp. Plasmid **18:**173–177.
28. **Nalin, R., P. Simonet, T. M. Vogel, and P. Normand.** 1999. *Rhodanobacter lindaniclasticus* gen. nov., sp. nov., a lindane-degrading bacterium. Int. J. Syst. Bacteriol. **49:**19–23.
29. **Olivera, F. L., R. C. Loehr, B. C. Coplin, H. Eby, and M. T. Webster.** 1998. Prepared bed land treatment of soils containing diesel and crude oil hydrocarbons. J. Soil Contam. **7:**657–674.
30. **Pelz, O., A. Chatzinotas, N. Anderson, S. M. Bernasconi, C. Hesse, W.-R. Abraham, and J. Zeyer.** 2001. Use of isotopic and molecular techniques to link toluene degradation in denitrifying aquifer microcosms to specific microbial populations. Arch. Microbiol. **175:**270–281.
31. **Rojas-Avelizapa, N. G., R. Rodriguez-Vazquez, R. Enriquez-Villanueva, J. Martinez-Cruz, and H. M. Poggi-Varaldo.** 1999. Transformer oil degradation by an indigenous microflora isolated from a contaminated soil. Resour. Conserv. Recycl. **27:**15–26.
32. **Salanitro, J. P., P. B. Dorn, M. H. Huesemann, K. O. Moore, I. A. Rhodes, L. M. Rice Jackson, T. E. Vipond, M. M. Western, and H. L. Wisniewski.** 1997. Crude oil hydrocarbon bioremediation and soil ecotoxicity assessment. Environ. Sci. Technol. **31:**1769–1776.
33. **Thompson, J. D., D. G. Higgins, and T. J. Gibson.** 1994. CLUSTAL W: improving the sensitivity of progressive multiple sequence alignment through sequence weighting, position specific gap penalties and weight matrix choice. Nucleic Acids Res. **22:**4673–4680.
34. **Venosa, A. D., M. T. Suidan, B. A. Wrenn, K. L. Strohmeier, J. R. Haines, B. L. Eberhart, D. King, and E. Holder.** 1996. Bioremediation of an experimental oil spill on the shoreline of Delaware Bay. Environ. Sci. Technol. **30:**1764–1775.
35. **Whiteley, A. S., and M. J. Bailey.** 2000. Bacterial community structure and physiological state within an industrial phenol bioremediation system. Appl. Environ. Microbiol. **66:**2400–2407.
36. **Yeom, S.-H., and A. J. Daugulis.** 2001. Benzene degradation in a two-phase partitioning bioreactor by *Alcaligenes xylosoxidans* Y234. Process Biochem. **36:**765–772.

Downloaded from http://aem.asm.org/ on May 9, 2021 by guest